Supporting Information

Hydrogen-Bonded Organic Frameworks-stabilized Charge Transfer Cocrystals for NIR-II Photothermal Cancer Therapy

Jiakang Tang[a][b] *Leihou Shao,*[a][b] *Ji Liu,*[a][b] *Qizhen Zheng,*[a][b] Xinyi Song[c], *Lanhua Yi*[c]* *Ming Wang*[a][b]*

[a] Jiakang Tang, Leihou Shao, Ji Liu, Qizhen Zheng, Prof. Dr. Ming Wang
Beijing National Laboratory for Molecular Sciences
CAS Key Laboratory of Analytical Chemistry for Living Biosystems
Institute of Chemistry, Chinese Academy of Sciences
Beijing 100190, China
E-mail: mingwang@iccas.ac.cn

[b] Jiakang Tang, Leihou Shao, Ji Liu, Qizhen Zheng, Prof. Dr. Ming Wang
University of Chinese Academy of Sciences
Beijing 100049, China

[c] Xinyi Song, Prof. Dr Lanhua Yi
Key Laboratory of Environmentally Friendly Chemistry and Applications of Ministry of Education, School of Chemistry, Xiangtan University, Xiangtan 411105, PR China
Email: yilanhua@xtu.edu.cn

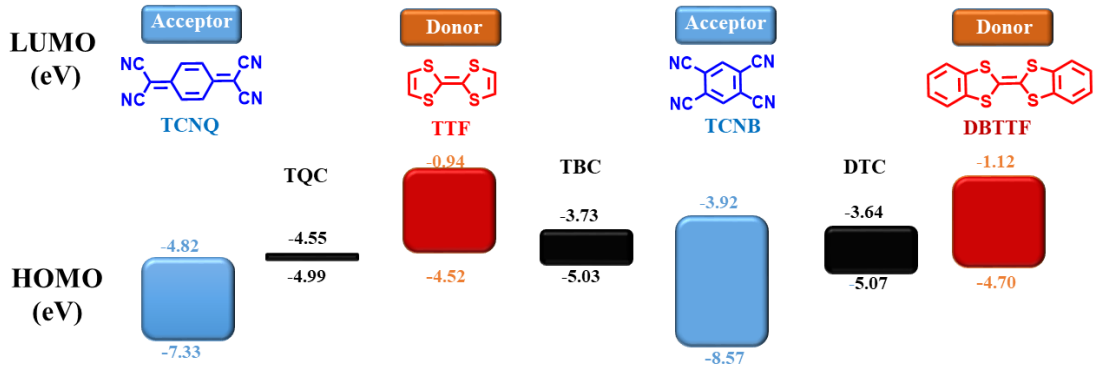

Figure S1 Schematic illustration of the HUMO-LUMO energy bandgap of the electron donor-acceptor pair used for self-assembling CT cocrystals.

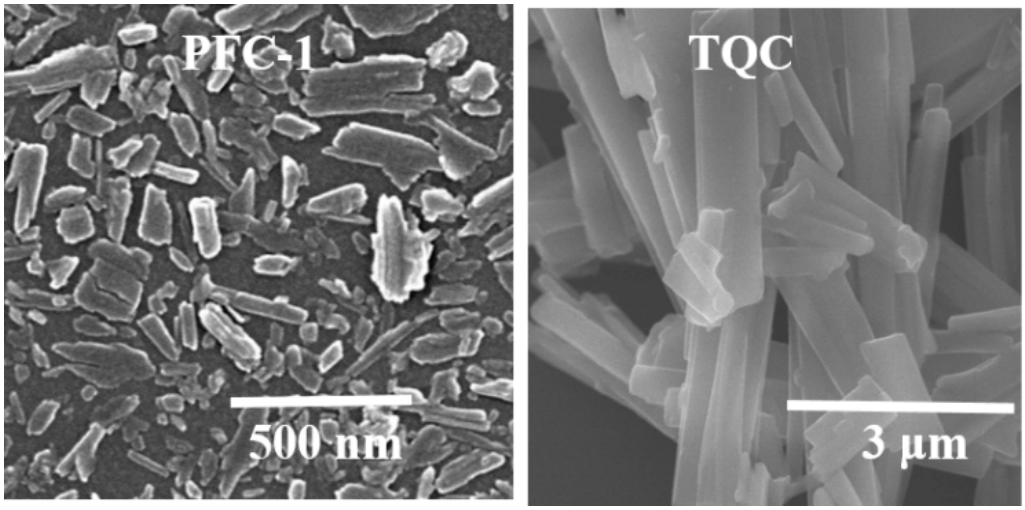

Figure S2 SEM images of PFC-1 and TQC.

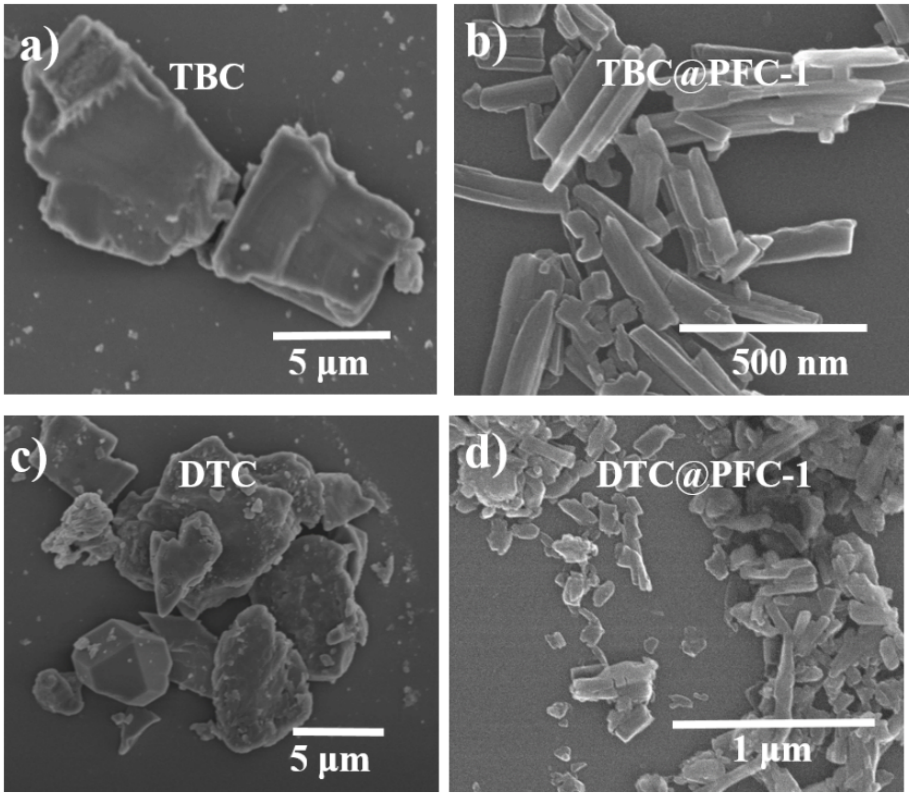

Figure S3 SEM images of TBC (a), TBC@PFC-1 (b), DTC (c) and DTC@PFC-1 (d).

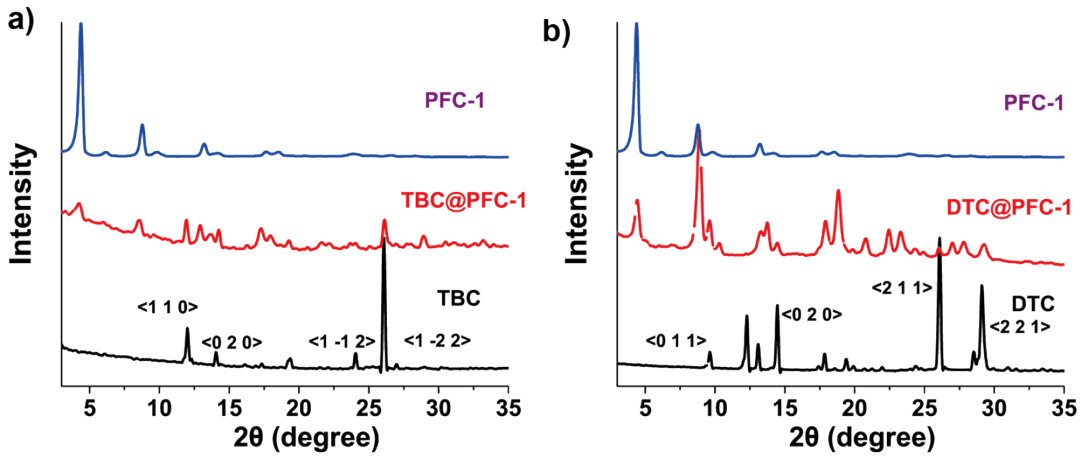

Figure S4 PXRD spectra of (a) PFC-1, TBC and TBC@PFC-1; (b) DTC and DTC@PFC-1.

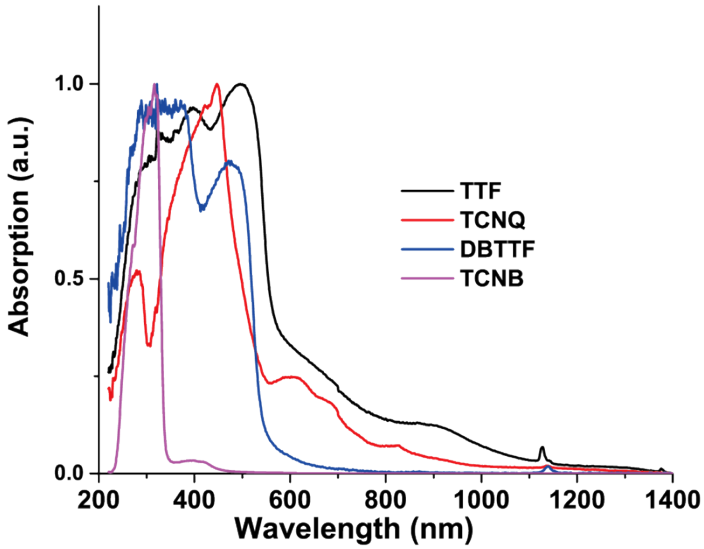

Figure S5 Solid-state absorption spectra of TTF, TCNQ, DBTTF and TCNB.

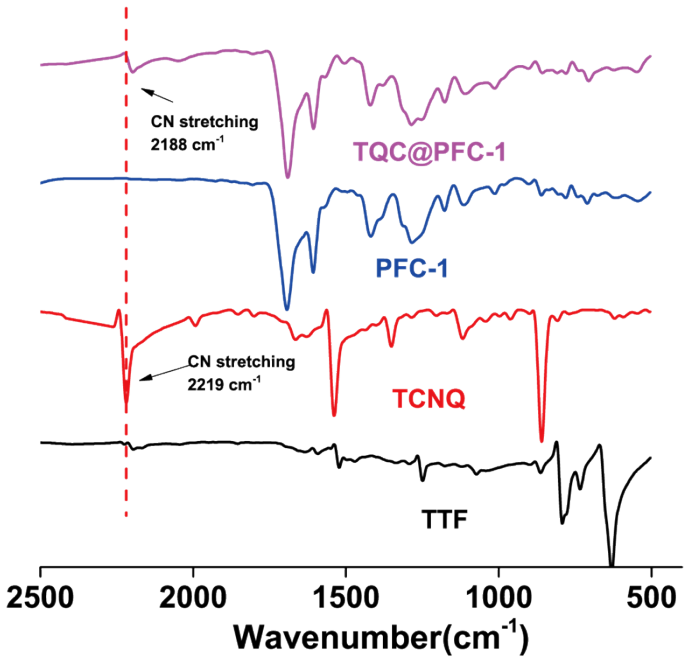

Figure S6 FT-IR spectra of PFC-1, TTF, TCNQ and **TQC@PFC-1**.

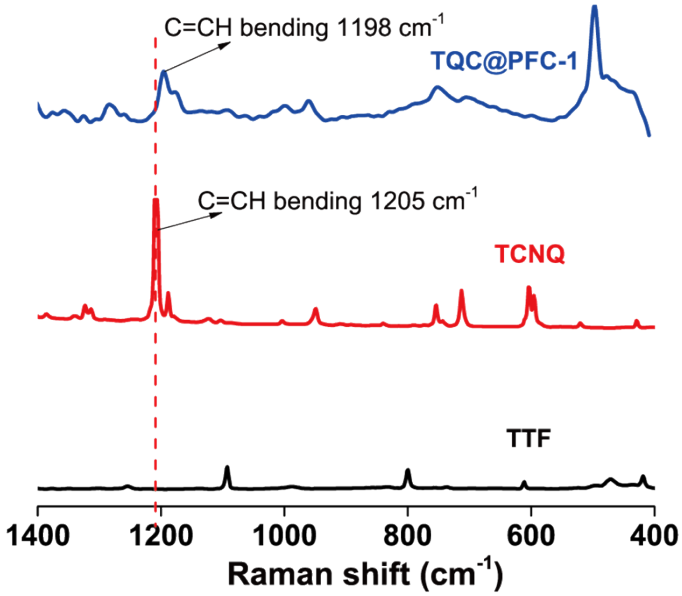

Figure S7 Raman spectra of TTF, TCNQ and **TQC@PFC-1**.

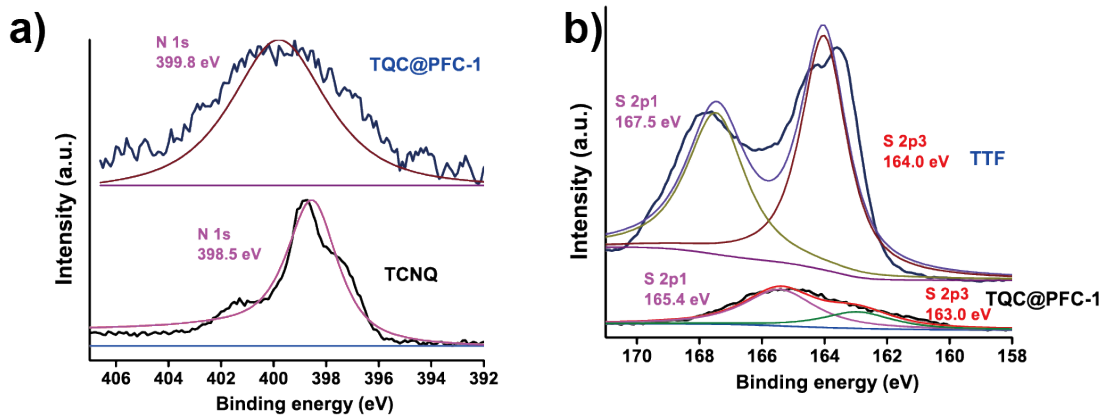

Figure S8 X-ray Photoelectron Spectroscopy measurements of **TQC@PFC-1**. a) N 1s spectrum of TCNQ and **TQC@PFC-1**. b) S 2p spectrum of TTF and **TQC@PFC-1**.

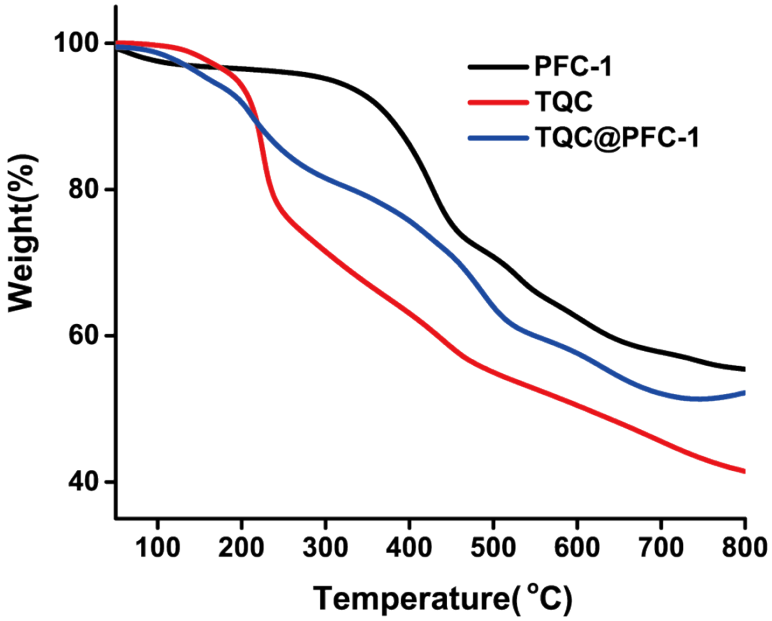

Figure S9 Thermogravimetric analyses of PFC-1, TQC and **TQC@PFC-1**.

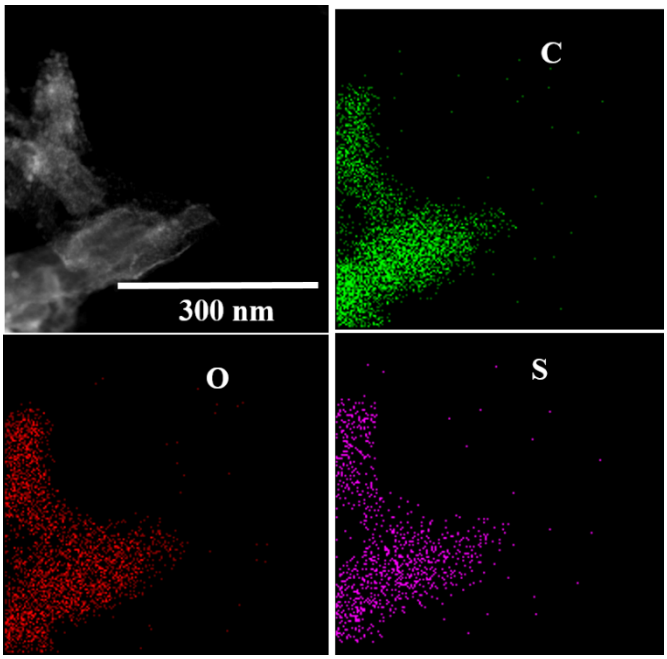

Figure S10 Transmission electron microscopy (TEM) image of **TQC@PFC-1** and the corresponding EDX mapping of C, O, and S.

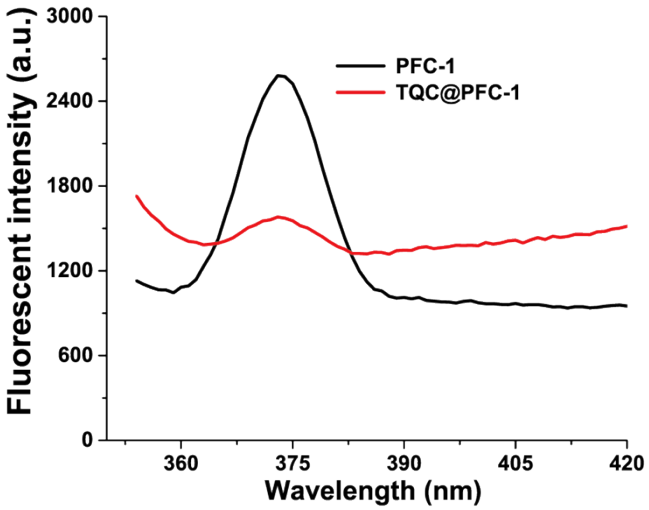

Figure S11 The fluorescent spectra of **PFC-1** and **TQC@PFC-1** (0.025 mg/mL). The fluorescence spectrum was measured by exciting the sample at 320 nm.

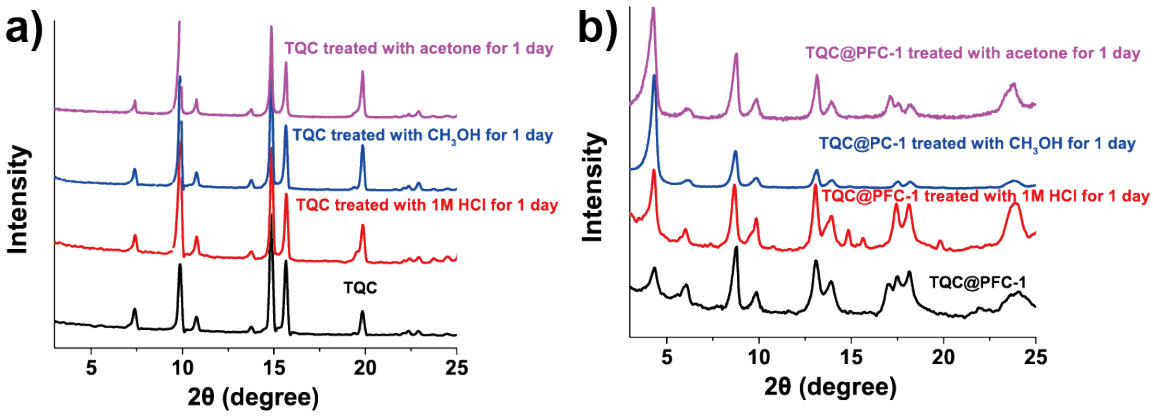

Figure S12 The PXRD patterns of TQC and **TQC@PFC-1** before and after incubation with acetone, CH_3OH, or 1 M HCl for 24 h.

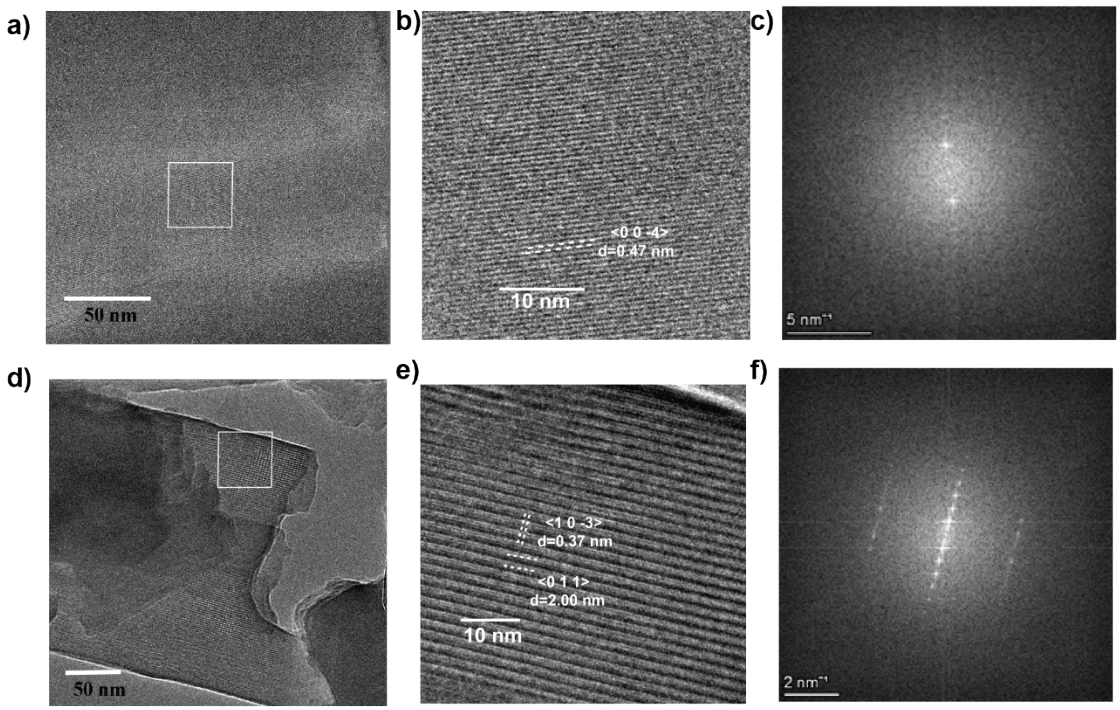

Figure S13 Structural profile of TQC and PFC-1 by cryo-TEM. a) Cryo-TEM image of TQC; b) The amplified cryo-TEM structure and c) the FFT pattern of the selected selected area highlighted in the white frame in a) . d) Cryo-TEM image of PFC-1; b) The amplified cryo-TEM structure and c) the FFT pattern of the selected selected area highlighted in the white frame in d)

Table S1 DLS characterizations of PFC-1, TQC and **TQC@PFC-1**.

Sample	**Size (nm)**	**Zeta potential(mV)**	**PDI**
PFC-1	228.9 ± 5.7	-32.9 ± 3.0	0.337
TQC	4380 ± 298	-29.2 ± 1.0	0.526
TQC@PFC-1	244.8 ± 20.5	-17.4 ± 1.4	0.188

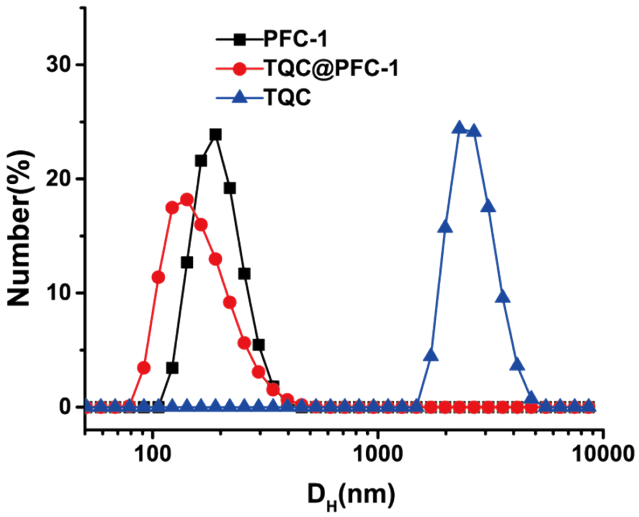

Figure S14 The size distributions of PFC-1, TQC, and **TQC@PFC-1** dispersed in water.

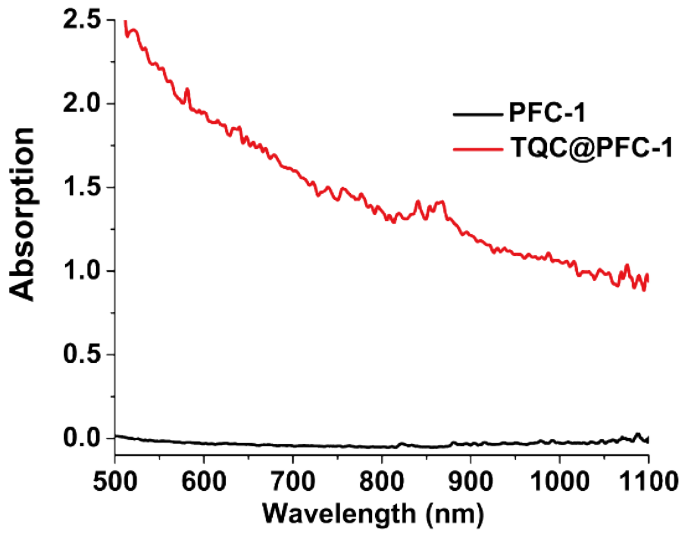

Figure S15 UV/Vis absorption spectra of aqueous solutions of PFC-1 and **TQC@PFC-1** (1 mg/mL).

The photothermal conversion efficiencies (η) were calculated using equations according to the previous method[1,2].

$$\eta = \frac{hs(Tmax - Tsurr)}{I(1 - 10^{-A1080})}$$

h is the heat transfer coefficient; s is the surface area of the container. I is the laser power and A is the absorbance at 1080 nm. Tmax and Tsurr are the maximum steady state temperature and the environmental temperature, respectively.

$$hs = \frac{mCwater}{\tau}$$

m is the mass of the solution containing the photoactive material, C is the specific heat capacity of the solution (Cwater = 4.2 J/(g•°C)), and τ is the associated time constant.

t=-τLn(θ)

θis a dimensionless parameter, known as the driving force temperature.

$$\theta = \frac{T - Tsurr}{Tmax - Tsurr}$$

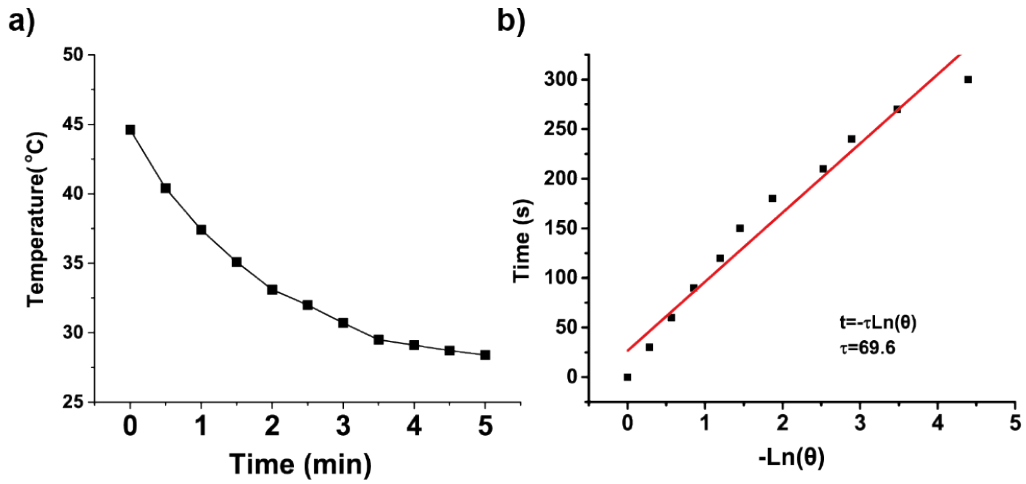

Figure S16 a) The cooling curve of **TQC@PFC-1** (1 mg/mL) after the irradiation of 1080 nm laser (0.8 W/cm^2) and b) its corresponding time-Inθ linear curve.

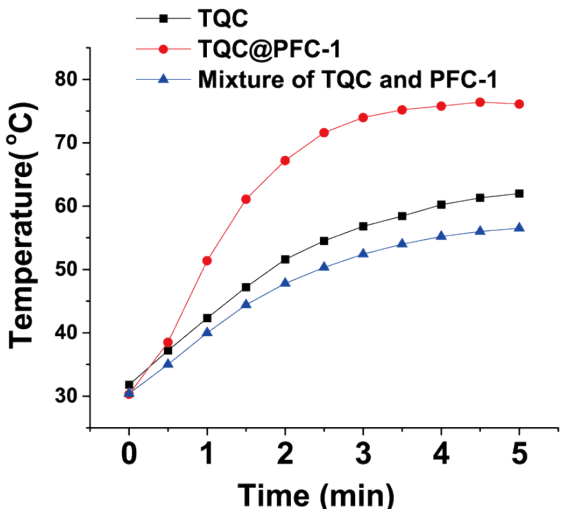

Figure S17 Comparison of the photothermal effect of TQC, physical mixture of TQC and PFC-1, and **TQC@PFC-1** aqueous solution (1 mg/mL) under 1080 nm laser irradiation (1.5 W/cm^2).

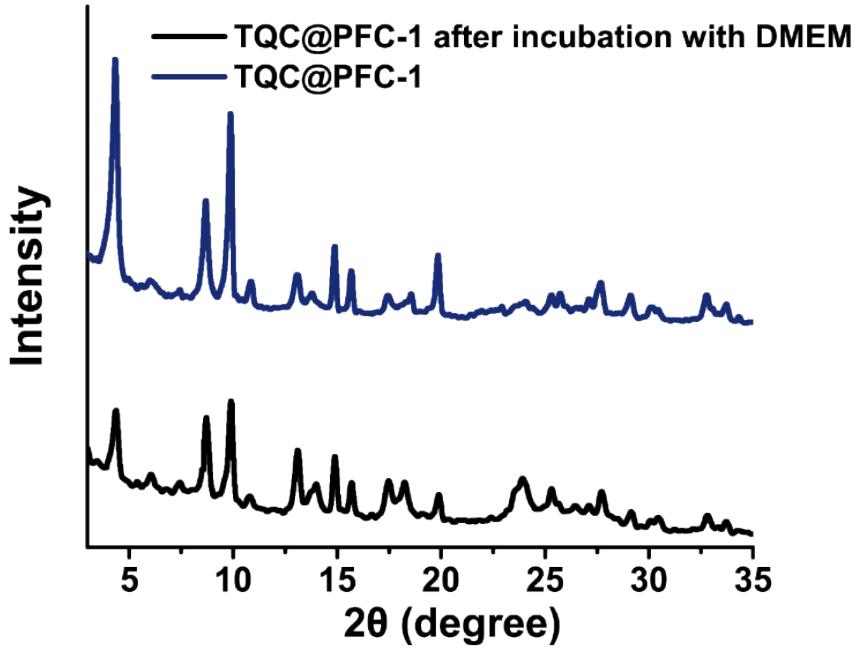

Figure S18 PXRD patterns of **TQC@PFC-1** before and after incubation with cell culture medium for 24 h

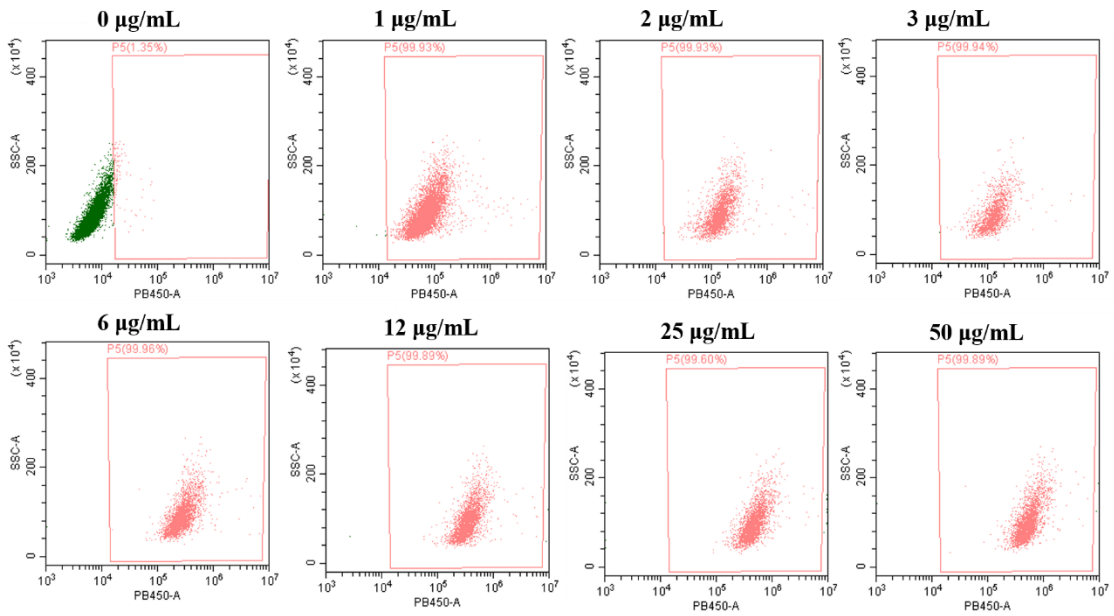

Figure S19 Flow cytometry analysis was performed to evaluate the delivery efficiency of **TQC@PFC-1**. HeLa cells were treated with varying concentrations of HOFs for 18 hours, followed by flow cytometry analysis to quantify PFC-1-positive cells.

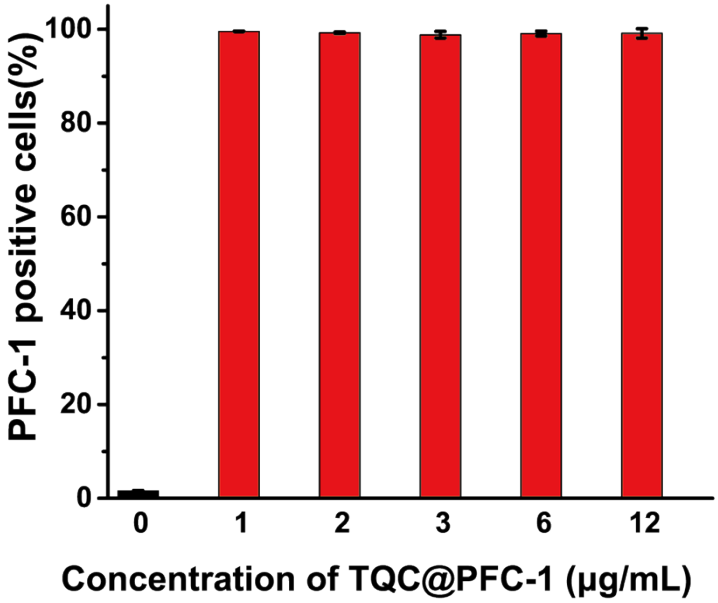

Figure S20 Cellular uptake study of **TQC@PFC-1** by HeLa cells. The cells were incubated with different concentrations of **TQC@PFC-1** for 18 h as indicated, followed by flow cytometry analysis to quantify PFC-1 positive cells. The data was presented as mean ± SD (n=3).

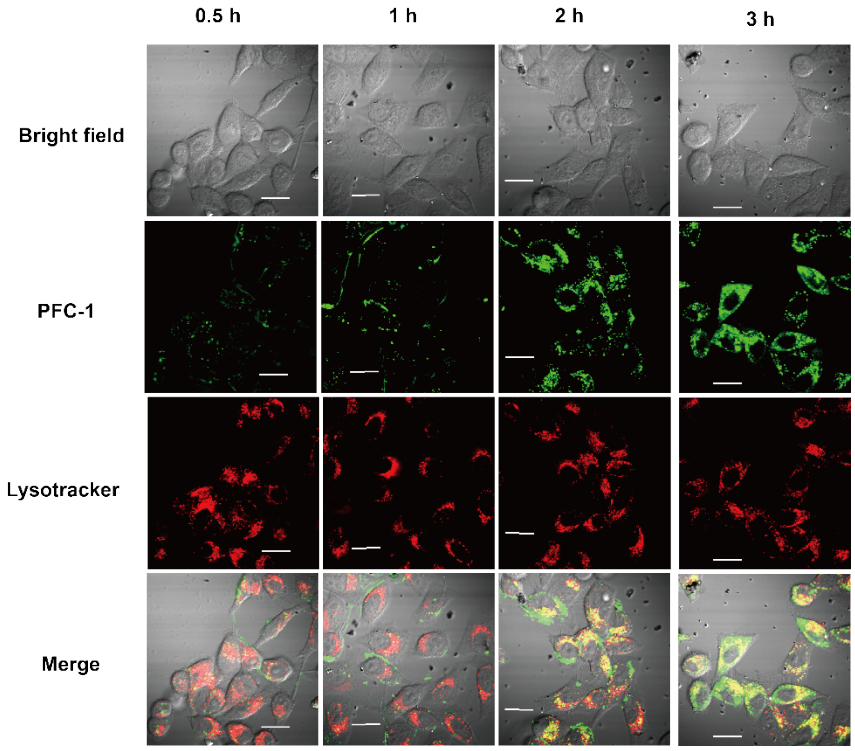

Figure S21 Confocal laser scanning microscopy (CLSM) images of HeLa cells incubated with 0.1 mg/mL **TQC@PFC-1** at different time points. The endosome/lysosome was stained with 100 nM LysoTracker@Red before CSLM imaging. Scale bar: 20 μm.

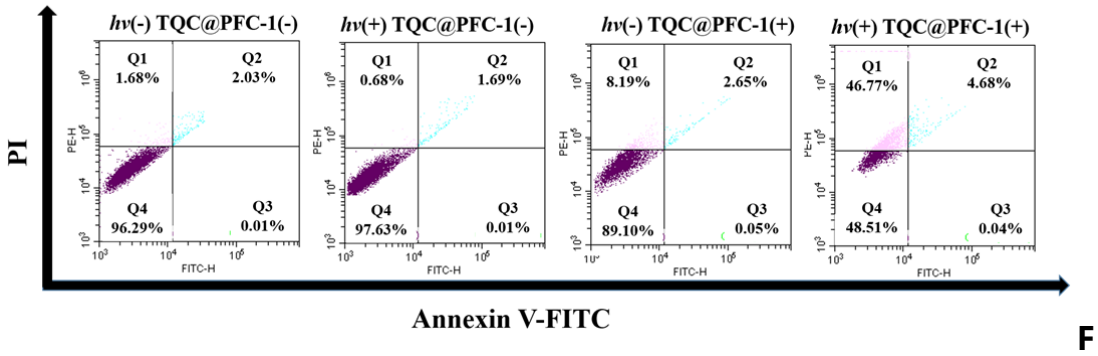

igure S22 The cell apoptosis assay was performed on HeLa cells treated with PBS or **TQC@PFC-1** with 1080 nm laser (1.5 W/cm^2) irradiation for 5 minutes.

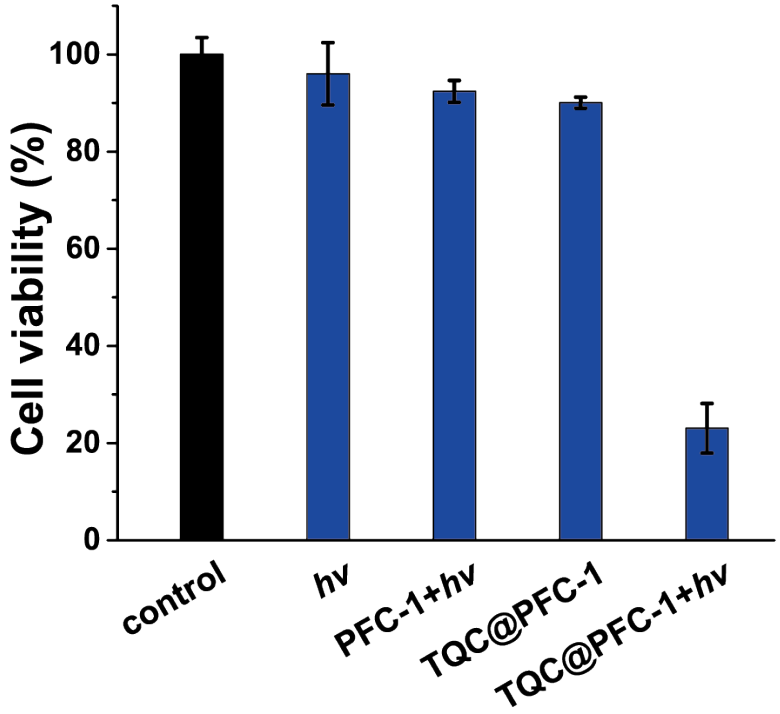

Figure S23 Photothermal ablation of B16F10 cells by **TQC@PFC-1**. The Viability of B16F10 cells treated with 0.2 mg/mL PFC-1 or 0.2 mg/mL **TQC@PFC-1** for 2 h, followed by light irradiation (1080 nm, 1.5 W/cm^2) for 5 min. as indicated. The differently treated cells were further incubated for 18 h before the determination of cell viability using MTT assay. The data was presented as mean ± SD (n=3).

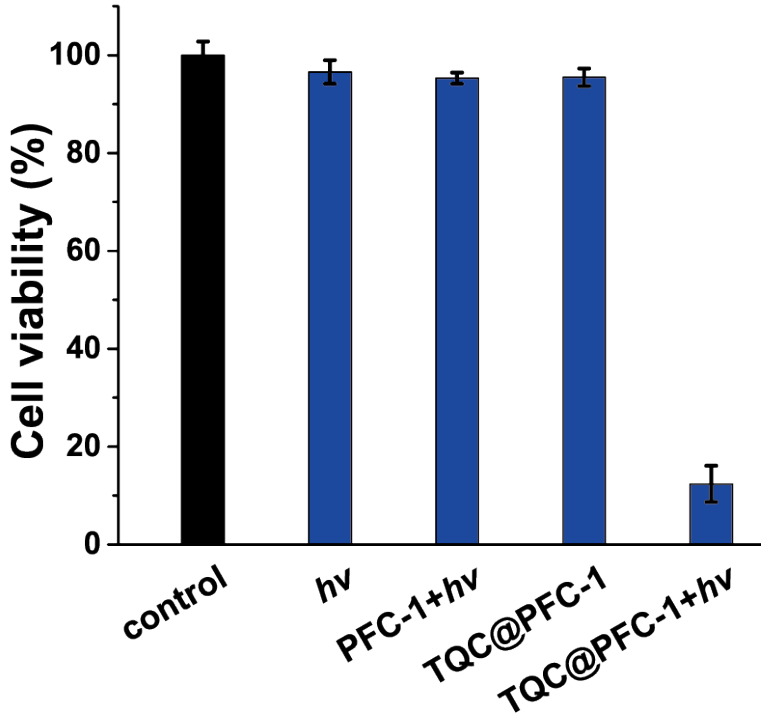

Figure S24 Photothermal ablation of 4T1 cells by **TQC@PFC-1**. The Viability of 4T1 cells treated with 0.2 mg/mL PFC-1 or 0.2 mg/mL **TQC@PFC-1** for 2 h, followed by light irradiation (1080 nm, 1.5 W/cm^2) for 5 min. as indicated. The differently treated cells were further incubated for 18 h before the determination of cell viability using MTT assay. The data was presented as mean ± SD (n=3).

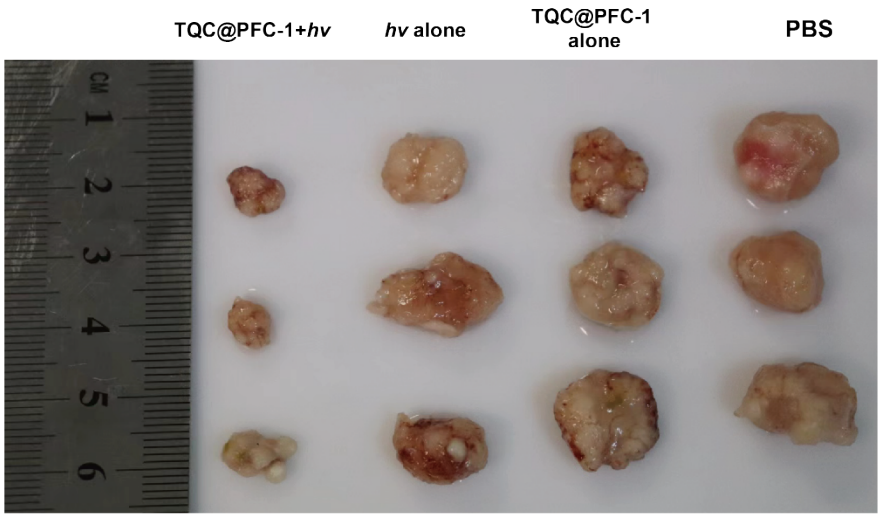

Figure S25 A representative image of tumors from four groups of mice after different treatments as indicated.

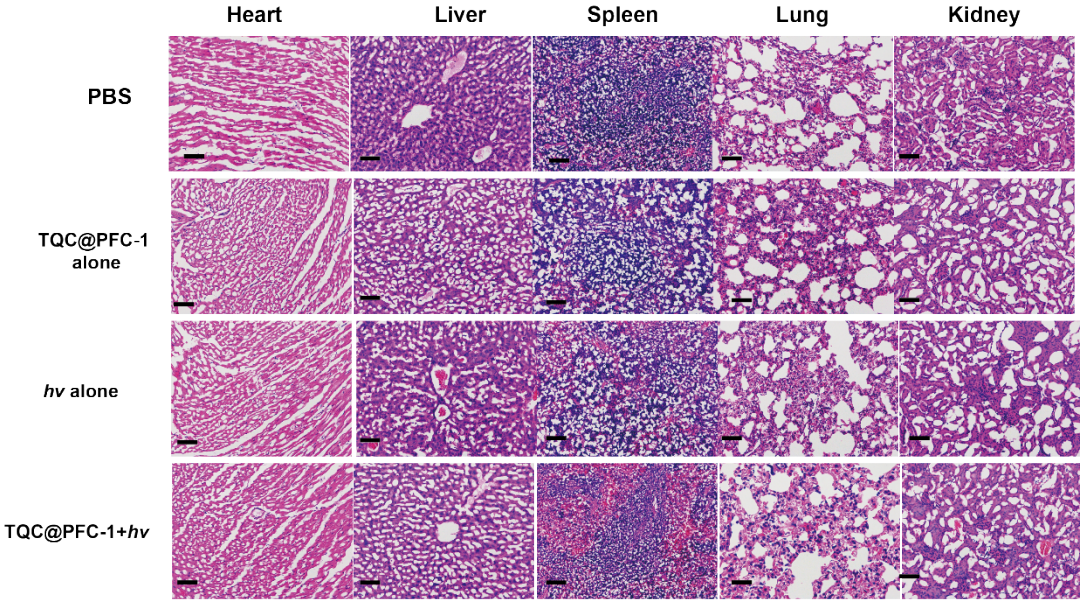

Figure S26 Histological hematoxylin and eosin (H&E) analysis of the major organs of mice received different treatments as indicated. Scale bar 200 μm.

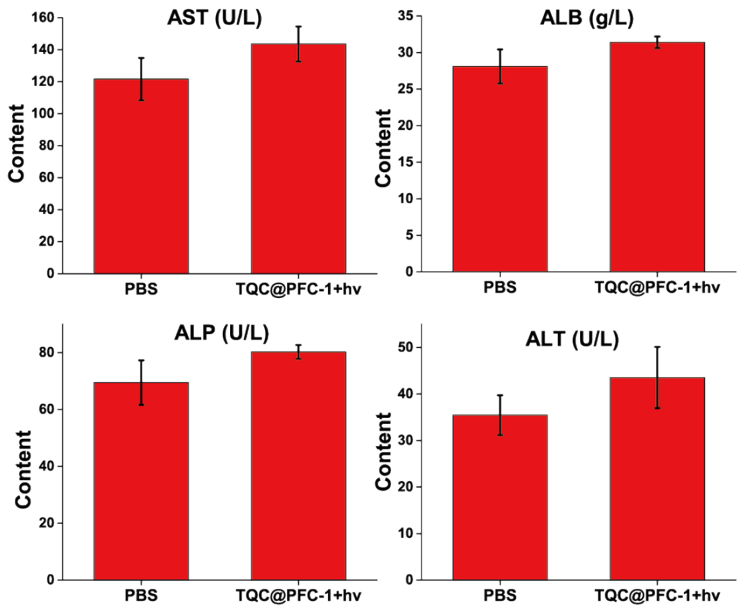

Figure S27 Liver function tests were performed on mice treated with **TQC@PFC-1** and laser irradiation.

Reference

1. Y. Wang, W. Zhu, W. Du, X. Liu, X. Zhang, H. Dong and W. Hu, *Angew. Chem. Int. Ed*. 2018, **57**, 3963-3967.
2. L. Zeng, L. Huang, Z. Wang, J. Wei, K. Huang, W. Lin, C. Duan and G. Han, *Angew. Chem. Int. Ed*. 2021, **60**, 23569-23573.